Sol−Gel Nanocoating: An Approach to the Preparation of Structured Materials

Rachel A. Caruso* and Markus Antonietti

Max Planck Institute of Colloids and Interfaces, D-14424 Potsdam, Germany

Received January 9, 2001

Nanocoating, the covering of materials with a layer on the nanometer scale, or covering of a nanoscale entity, to form nanocomposites and structured materials using the sol−gel process is reviewed. Templates from spherical nanoparticles to complex bicontinuous networks are discussed where either the coated material or the structured inorganic hollow frame resulting after removal of the template are of interest in fields of application ranging from information storage to catalysis. The sol−gel procedure allows coating of templates with complex shapes on the micrometer to nanometer scale, which some commonly used coating procedures cannot achieve. In addition, sol−gel coating techniques can be applied to delicate systems without disruption of their structure or functionality, for example, the coating of biocomplexes or organic aggregates, such as organogelators. Three-dimensional structures with elaborate pore architectures, such as polymer membranes and gels, can also be infiltrated with sol−gel solutions to achieve nanocoatings.

1. Introduction

The sol−gel process involves inorganic precursors (a metal salt or organometallic molecule) that undergo various reactions resulting in the formation of a three-dimensional molecular network. A common example is the hydrolysis and condensation reactions of metal alkoxides to form larger metal oxide molecules:

Hydrolysis:

$$M(OR)_4 + H_2O \rightarrow HO-M(OR)_3 + ROH \cdots\rightarrow M(OH)_4 + 4ROH$$

Condensation:

$$(OR)_3M-OH + HO-M(OR)_3 \rightarrow (RO)_3M-O-M(OR)_3 + H_2O$$

$$(OR)_3M-OH + RO-M(OR)_3 \rightarrow (OR)_3M-O-M(OR)_3 + ROH$$

where M represents the metal and R the alkyl group. A comprehensive overview of the sol−gel process can be found in the book by Brinker and Scherer.[1]

Coating is simply the act of covering a material with a layer; hence, nanocoating is either to cover with a layer on the nanometer scale or to cover a nanoscale entity. A nanocomposite is comprised of a combination of two or more different substances of nanometer size, thereby producing a material that generally has enhanced or specific properties due to the combined properties and/or structuring effects of the components. The material on which the coating is made, which therefore influences the structure, is called the template. The template can be removed from the composite material, leaving a substance with interesting structural properties.

A differentiation between coating and casting must be made, as is depicted in Figure 1. The process of using a template to make a reverse replica or even a replica, with similar overall morphology to the mold itself, is called casting. Sol−gel processes are often used in casting techniques for the formation of hybrid materials as well as ceramics with controlled morphology after removal of the template. Because this review focuses on nanocoating, this related technique of casting is not discussed further, but the interested reader is referred to the literature.[2−20]

Materials are coated for a number of reasons: Coatings can make a substance biocompatible, increase a material's thermal, mechanical, or chemical stability, increase wear protection, durability, or lifetime, decrease friction or inhibit corrosion, or change the overall physicochemical and biological properties of the material. There are numerous coating procedures that are widely used including vapor deposition, plasma-assisted/ion-beam-assisted techniques, chemical reduction, pulsed laser deposition, mechanical milling, magnetron sputtering, self-assembly, layer-by-layer coating, dip coating, sol−gel coating, TUFT (tubes by fiber templating) process,[21] and electrochemical deposition. The majority of these techniques is preferentially used to coat planar substrates. However, when more complex shapes require coating, and when these materials are on the nanometer to micrometer scale, many of the aforementioned techniques have serious drawbacks. In this case the sol−gel process, which can be carried out in solution, is attractive.

Coating in solution is generally performed using either precursor molecules or preformed particles to form the layer. Electrostatic interactions, hydrogen bonding, and covalent bonding are some of the associat-

* To whom correspondence should be addressed. E-mail: Rachel.Caruso@mpikg-golm.mpg.de. Fax: +49 331 567 9502.

10.1021/cm001257z CCC: $20.00
Published on Web 07/06/2001

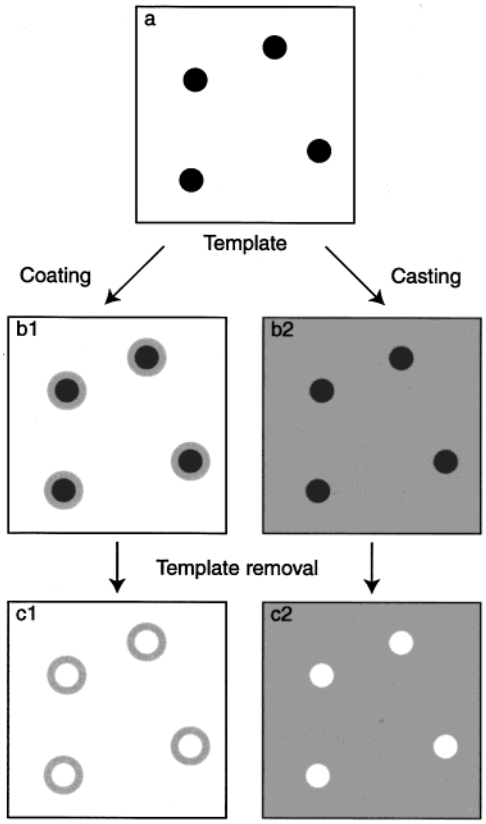

Figure 1. Schematic showing the following: (a) the initial template; (b1) *coating* of the template; (b2) *casting* of the template; (c1) and (c2) the material that remains after the removal of the template.

ing forces between the coating and the material being coated. Coating procedures that begin with preformed nanoparticles as the coating material can be found in refs 22−30.

This article will review recent sol−gel coating procedures applied to nanomaterials. Beginning with colloid nanoparticle templates (part a in Figure 2), which are (unidimensional) nanoscaled along all axes, to elongated objects (nanoscaled in two dimensions and sometimes micrometer-scaled in the third) such as carbon nanotubes, fibers, and crystals (part b in Figure 2), and then bicontinuous nanostructured networks (part c in Figure 2) such as polymer gels. Although a broad overview of different templates is given, it is not an exhaustive compilation of the literature.

An attractive supplement to the formation of nanocomposites is the interesting structures that can be obtained upon removal of the initial template, such as hollow spheres, hollow fibers, and three-dimensional hollow frames (scaffolds). These porous structures will also be discussed as they are found to have applications as catalysts and supports and in separation technology.

2. Colloid Particles

Colloid particles are often coated to alter the surface properties of the particles, such as adding a specific charge or functionality, thereby changing or having an influence on their stability. Such coatings can widen the areas of application or enhance the use of particles in certain areas.

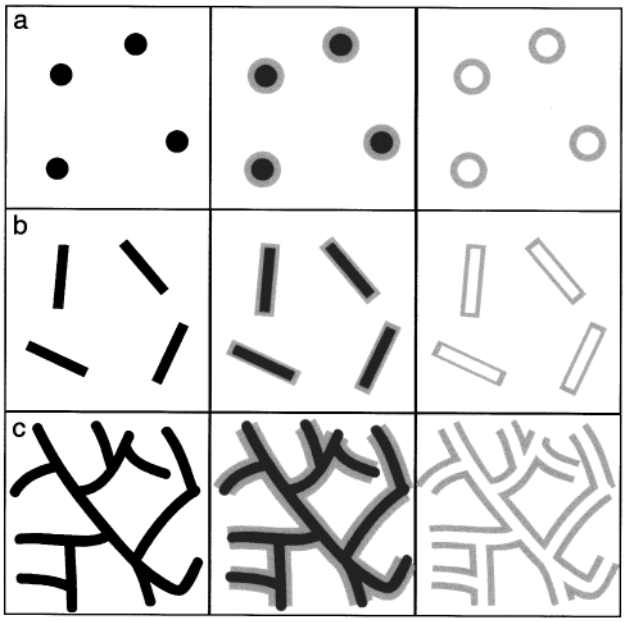

Figure 2. Schematic that shows from left to right the initial template, the coated composite material, and then the hollow inorganic structures formed upon removal of the template for (a) nanoparticles, (b) crystals, and (c) bicontinuous networks.

2.1. Inorganic Particles. Monodisperse silica spheres with magnetic cores were formed by silica precipitation from an aqueous sodium silicate solution onto magnetite nanoparticles.[31] Magnetite particles have an isoelectric point of pH ∼ 7, hence, colloidal stability is problematic in aqueous solutions around neutral pH, making silica coating favorable for reasons of stability. Coating with silica lowers the isoelectric point to ≈3, thereby increasing the aqueous ferrofluid stability at near neutral pH. Also, in nonaqueous solutions aggregation can occur, and a chemically bound, hence nondesorbing, surface layer can prevent aggregation. To achieve this coating, a silicate solution was mixed with tetramethylammonium hydroxide stabilized magnetite particles (diameter of ≈10 nm) and slowly titrated with HCl to a pH of 10. After dialysis and centrifugation to remove soluble sodium silicates and aggregated magnetite particles, the coated particles had an isoelectric point of pH = 3.3, and elemental analysis demonstrated the presence of silicon from which the film thickness of 0.5 nm was estimated. Further coating was achieved by dispersing these thinly coated particles in ethanol, ammonia, and tetraethoxysilane (TEOS) and stirring for 1 day at 20 °C. This seeding procedure gave particles with a final diameter of 68 nm, containing single magnetite cores. Further surface modification of the coated particles with ((3-methacryloxy)propyl)trimethoxysilane or octadecyl alcohol afforded coated magnetite particles that were dispersible in organic solvents.

Silica coatings have been achieved on gold nanoparticles, Au@SiO_2, not only to stabilize the particles but also to modulate their optical properties.[32] (Liz-Marzán et al. introduced the Au@SiO_2 nomenclature to signify gold cores coated with a silica shell.) Gold particles (15 nm in diameter) prepared by citrate reduction of $HAuCl_4$ were coated with (3-aminopropyl)trimethoxysilane, which complexed via the amine groups to the gold surface, displacing the previously adsorbed citrate ions. The

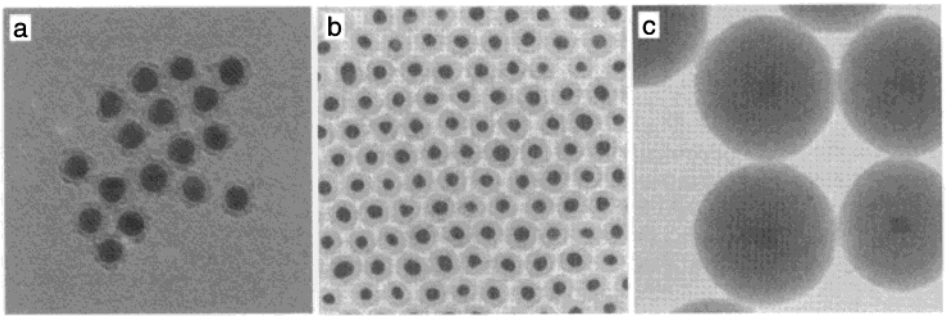

Figure 3. Transmission electron micrographs of 15-nm gold particles coated with silica layers of a thickness of (a) ≈2 nm, (b) 10 nm, and (c) 83 nm. Reprinted in part with permission from ref 32. Copyright 1996 American Chemical Society.

formation of just a monolayer of this primer layer was important to prevent flocculation of the particles. Upon the addition of a sodium silicate solution to the sol, the silanol groups of the primer layer then acted as anchor points for the formation of a thin silica layer (2−4 nm) around the particles. Figure 3a shows a transmission electron microscopy (TEM) image of the thin layer formed 42 h after the addition of the silicate. The coated particles could then be transferred into ethanol or ethanol/water mixtures to increase the silica layer thickness by the slow condensation of TEOS, as seen by TEM in Figure 3b,c. This procedure has been adapted for the coating of CdS nanoparticles, CdS@SiO_2, by the use of a 3-(mercaptopropyl)trimethoxysilane primer layer.[33] Contrary to the citrate stabilized cadmium sulfide particles, which photodegrade through photochemical oxidation, the presence of the silica coating suppresses oxidation.

Because of the control of the silica shell thickness, which allows tuning of the intercore distance in dense films, these core/shell materials can be used for the construction of ordered two- and three-dimensional assemblies with special optical properties.[34] Thin films of coated nanoparticles have been formed with control over the intercore distance.[34−36] The optical effect due to the controlled coupling of the nanoparticle dipoles of Au@SiO_2 with different silica-coating thickness is demonstrated by the variation in film color in Figure 4. The silica shells have been shown to be porous by the addition of iodine, a strong oxidant, to silica-coated (10-nm-thick) silver particles, Ag@SiO_2: Oxidation of the silver to silver iodide deposited outside the shell was monitored and observed by absorbance spectroscopy and transmission electron microscopy, respectively.[37] Hollow silica nanocapsules could be formed by exposing silica-coated (10-nm-thick) gold particles to cyanide.[37]

The primer layer is not always necessary for the coating of metal particles with metal oxides; 15-nm gold particles were coated by adding fresh sodium stannate to a gold sol at pH 10.5.[38] The tin dioxide deposited on the gold surfaces as 1-nm nuclei, which upon heating produced stable cassiterite-coated gold particles, Au@SnO_2. These coated particles have been shown to have advantageous capacitor properties over noncoated gold particles. Because of the large difference between the Fermi levels of the core and shell, such particles have potential applications as electron storage and electronic circuit components. Titanium dioxide-coated silver nanoparticles, Ag@TiO_2, were produced in a one-pot procedure by refluxing a mixture of titanium butoxide and acetylacetone in ethanol and silver nitrate

Figure 4. Photographs of dense Au@SiO_2 films with 15-nm-diameter core gold particles and different shell thicknesses. The top left film is a sputter-coated gold film. The next two bluish films are formed from gold sols that have sodium citrate (0.5 nm) and sodium mercaptopropionate (1.0 nm) shells; the other films utilize gold colloids with silica shells having thicknesses 1.5, 2.9, 4.6, 12.2, and 17.5 nm. The shell thickness controls the dipole coupling between particles and hence the color of the film. Reprinted with permission from ref 34. Copyright 2000 The Royal Society of Chemistry.

in *N*,*N*-dimethylformamide and H_2O.[39] Thin films of these coated particles are formed, and even in this close-packed configuration, the nanoparticles remain electrically insulated as the surface plasmon band of the coated silver particles in the layers remained the same as that of the sol.

Silica was also coated on nanosized silver particles using the Stöber method[40] without surface pretreatment.[41] The silver sol was diluted with 2-propanol before the addition of water and ammonia. Once the temperature had stabilized at 40 °C, TEOS was added rapidly and the reaction continued for varying periods of time. Smooth, homogeneous coatings were achieved after 2 h with the silica layer thickness increasing to 80 nm.

Granular or smooth coatings were obtained, depending on reactant concentrations.

A different approach that makes use of a microemulsion reaction matrix for the formation of coated nanoparticles has also been documented. Copper, silver, and cadmium sulfide particles have been coated with silica, and cadmium sulfide also with titania, by hydrolysis and condensation of the respective alkoxide precursor within the microemulsion matrix.[42] In these examples the nanoparticle formation as well as the coating procedure are performed within the microemulsion. Taking the coated silver as an example, the formation of the silver nanoparticles in the microemulsion droplets gave some control over the size of the particle by varying the water/surfactant ratio.[43] The water to TEOS ratio influenced the thickness of the SiO_2 coating. The silica-coated silver particles are monodisperse and spherical with diameters between 25 and 30 nm. However, some nonfilled silica particles were also produced. Optical electronics is a potential area of application for the coated metal and metal sulfide particles.

Silica coatings on larger colloids have also been obtained. Titania (diameter, 1 μm) and zirconia (100 nm) colloids were coated by hydrolysis of tetramethoxysilane in ethanol/ammonia solutions, giving a silica coating thickness of 25 and 10 nm, respectively.[44] These coated particles were used as traceable mineral colloids for transport experiments.

Matijević and co-workers fabricated numerous combinations of submicrometer-sized core/shell particles, with the core material varying in morphology from spherical to elongated. Spindle-shaped hematite was coated by zirconium hydrous oxide by aging zirconium sulfate solutions in the presence of formamide and preformed hematite at 70 °C for 2 h.[45] Manipulation of the layer thickness was achieved by changing the concentration of core particles and coating solution. The addition of formamide, which upon heating decomposes to release NH_4^+ ions, increased the pH, enhancing hydrolysis. The initial zirconium hydrous oxide coating was amorphous, but upon heating tetragonal zirconium dioxide was formed. Hematite cores were also coated with yttrium carbonate,[46] chromium hydrous oxide,[47] silica,[48] and manganese compounds.[49]

Titania coatings on monodisperse silica particles were obtained using a titanyl sulfate precursor in sulfuric acid.[50] Coating uniformity was dependent on solution pH, the concentration of silica powder, the rate of titanyl sulfate addition, and the total reaction volume. Two-step processes, involving the double addition of the titanyl sulfate solution with filtration between, increased the coating layer thickness and uniformity and prevented particle aggregation. Zinc oxide cores[51] and copper(II) basic carbonate spherical particles[52] were coated with titania layers by controlled hydrolysis of titanium butoxide in ethanol solutions. Upon heating of the latter, crystallization to CuO and titania (both anatase and rutile phase) occurred. Zirconium basic sulfate particles could also be coated with yttrium compounds by aging solutions of the $Zr_2(OH)_6SO_4$ aqueous dispersions in the presence of yttrium nitrate and urea at 90 °C for 2 h.[53] Both silica-coated yttria and yttria-coated silica have also been prepared by precipitation techniques.[54]

Titania-coated silica spheres have received a lot of attention because of their potential use in catalytic, pigment, and photonic crystal applications. Silica microspheres (diameter, 270 nm) have been coated with titania monolayers[55] using titanium *tert*-butoxide in tetrahydrofuran under nitrogen and multilayers[56] using titanium *n*-butoxide in ethanol. Coating thicknesses of submonolayer to 7 nm of amorphous titania were achieved; upon calcination, polycrystalline anatase coatings were found. Control of precursor and water concentrations was essential for preventing precipitation of titania particles and aggregation of the coated particles. Developing this process to a multistep method on larger monodisperse spheres (diameter, 550 nm) gave a coating thickness of 46 nm after five repeated deposition steps.[57]

Micrometer-sized iron particles were coated with silica by hydrolysis of TEOS after priming of the surface with gelatin.[58] The iron particles were first heated at 80 °C in a 1% aqueous solution of gelatin until the solvent evaporated and the system dried, and then it was aged at 120 °C for 24 h before being added with ammonia and water to 2-propanol at 20−40 °C and stirred for 1 h. TEOS was added and the sample aged for 1−24 h. The gelatin interacts through both nitrogen and oxygen with the iron particle surface and binds to the silica. Thicknesses of 20−100 nm could be achieved. This silica coating increased the temperature of oxidation of the iron particles from 330 to 400 °C.

2.2. Polymer Spheres. Polymer spheres have been coated with a variety of inorganic materials. As polymer spheres are accessible with low size distribution and in a variety of compositions, they are attractive templates. Coatings are commonly applied with the intention to remove the core; that is, the organic material is often used as a sacrificial template to form structured inorganic materials such as hollow spheres.

Matijević and co-workers have modified their coating procedure for inorganic templates to coat polymer spheres. Basic yttrium carbonate layers were deposited onto polystyrene (PS) latex by the addition of yttrium nitrate, urea, and poly(vinylpyrrolidone) (PVP) and aging at 90 °C for 2 h before quenching in cold water.[59] The yttrium carbonate layer coating the PS particles can be seen in the transmission electron microscopy image in Figure 5. To prevent precipitation of yttrium carbonate, the ratio of core to yttrium nitrate had to be controlled. The yttrium carbonate was found to coat positively charged latex but not negatively charged latex. Control of the thickness and morphology of the layers depended on the reactant concentrations, aging time, and temperature. Aging both cationic and anionic PS latex in the presence of zirconium sulfate, formamide, urea, and PVP led to zirconium compound coatings on the latex particles.[60] A suggested mechanism was the heterocoagulation between the latex spheres and in situ precipitated inorganic particles. Calcination of the hybrid gave hollow inorganic spheres.

As most metal alkoxide precursors rapidly undergo hydrolysis and condensation in the presence of water, coating in nonaqueous solvents is preferable. Amorphous titanium dioxide coatings on PS particles have been achieved by the hydrolysis of titanium tetrabutoxide by working in ethanolic solutions.[61] Seeded

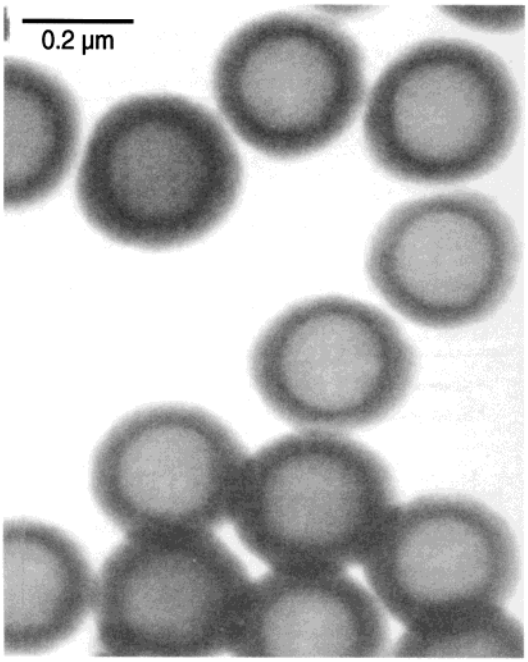

Figure 5. Yttrium carbonate coating on cationic polystyrene particles. Reprinted in part with permission from ref 59. Copyright 1990 Academic Press.

polymerization of TEOS on the surface of 2.3-μm polystyrene spheres (as well as free silica particle formation) has also been attained.[62] After centrifugation and drying, the coating step could be repeated. An increase in the silica nanoparticle (30−40 nm in diameter) coating from 7.8 to 18.5% (w/w) was obtained after one and three coatings, respectively. Bamnolker et al.[62] formed noncontinuous coatings consisting of crystallized Fe_3O_4 nanoparticles (30−40 nm) on the microspheres by increasing the pH of an iron chloride tetrahydrate aqueous solution in the presence of sodium nitrite at 60 °C under N_2. During the coating the microspheres became brown-black in color. Silica coating of these iron oxide-coated PS particles added stability to the iron oxide coating as leaching occurred at high and low pH. Hollow silica and magnetic silica spheres could be obtained after calcination. Such hollow materials may be of importance to areas such as fillers, pigments, and ultrasonic contrast agents.

Macroporous materials prepared by infiltrating colloidal crystals of either polymer or silica spheres with precursor molecules or nanoparticles have lately received attention.[63−70] The formation of such macroporous materials are not further considered here as they generally yield either incompletely coated individual spheres (thereby producing windows where the spheres come in contact) or a cast of the colloidal crystal. Zhong et al., however, have used colloidal crystals to coat individual polymer spheres.[71] A crystalline array of polystyrene spheres was fabricated by drying the latex between glass substrates. Infiltrating the crystal with sol−gel precursor solutions leads to sphere separation, and upon exposure to air, the gel precipitated, forming a homogeneous, thin coating on the spheres. The thickness of the coating was dependent on the concentration of the sol−gel solution. Titania and tin oxide-coated polystyrene spheres have been produced using this method. The optical and electrical properties of such materials will determine their areas of application.

3. Crystals

Two crystal types are discussed in this section, inorganic metal salt crystals and organic tartrate and oxalate crystals. While the metal salt crystal yields inorganic tubes containing metal nanoparticles, the organic material can be dissolved or decomposed, leaving inorganic tubes with the inner channel shaped by the crystal.

3.1. Metal Salt Crystals. A novel approach to the formation of metal oxide nanotubes containing metal particles with high metal content has been carried out by Hippe et al.[72] This procedure consists of the sol−gel synthesis of silica and titania in the presence of platinum salt crystals. Platinum tetraammine hydrogen carbonate precipitates in ethanol forming monoclinic crystals that have a rectangular cross section. Ion exchange between the hydrogen carbonate and the deprotonated silicate species as well as hydrogen bonding between the amine ligands and the silicate were assumed to take place at the surface of the metal salt crystal, thereby anchoring the silicate to the crystal. Upon calcination of the coated crystals at 500 °C, decomposition of the salt and reduction of the platinum occurred, resulting in rectangular metal oxide nanotubes containing platinum metal particles (Figure 6). The inner diameter ranged from 10 to 300 nm and the length from a few nanometers to 3 μm. For the formation of platinum within titania hollow tubes nonstructured titania was also found in solution because of the rapid hydrolysis and condensation rates of the alkoxide precursor. Transmission electron microscopy images showed platinum particles on the outer surface of the tube. Optimization is required to rectify the variation in final tube size by control of the crystal formation and to evenly distribute the metal particles within the tubes. Nanoelectronic devices could make use of such well-formed nanowires.

3.2. Organic Crystals. The formation of hollow silica tubes in aqueous solution in the presence of DL-tartaric acid was first reported by Nakamura and Matsui.[73,74] These silica tubes have been shown to form using surface-specific sol−gel polymerization on organic crystal templates.[75] TEOS was added to ammonium DL-tartrate in ethanol and the solution was left standing (30 min). Upon the addition of base, a white precipitate was formed that consisted of flexible, smooth-surfaced, open-ended, amorphous silica tubes with wall thicknesses of 30−300 nm. The tubes had a length of 200−300 μm, a width of 0.1−1 μm, and inner dimensions of 200−800 nm. The tube size could be increased by adding base to the solution prior to TEOS. The organic crystals form upon the addition of base in ethanol solution; therefore, the silica tubes are formed by specific deposition of the inorganic material on the external crystal surface. The crystals, being soluble in water, were dissolved during the condensation reactions or washing procedure, leaving stable hollow inorganic structures shaped by the crystal. Using the in situ formation of ammonium oxalate crystals in water, silica tubes with 300-nm-thick walls and lengths of 50−100 μm with

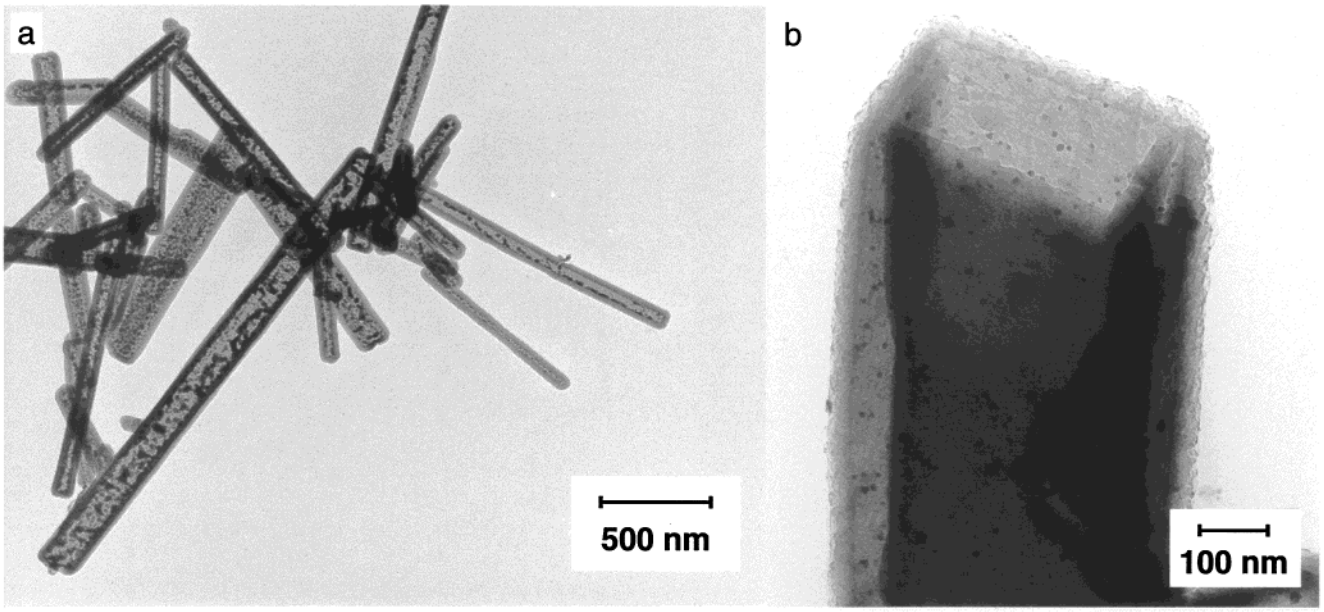

Figure 6. TEM micrographs of (a) calcined SiO_2 nanotubes (the dark spots represent platinum particles) and (b) showing the marked rectangular cross section of the SiO_2 nanotube. Reprinted with permission from ref 72. Copyright 1999 Elsevier Science.

rectangular- or triangular-shaped channels 0.7−6.5-μm wide could also be formed.[75]

4. Fibers

Recently, fibers, both of inorganic and organic nature, have been coated using sol−gel processes. Alumina and silica−alumina fibers, diameters of 10 or 15 μm, respectively, have been coated with ceria by infiltrating the fibers with a cerium nitrate solution before thermal decomposition at 400 °C to form a cerium oxide layer.[76] The ceria layer consisted of particles 200−400 nm in size. The coating was required to prevent sintering between individual fibers. Synthesis of zeolite A on cellulose fibers was achieved by immersing the fibers in an aluminosilicate gel, which led to zeolite crystallization after 4.5 h at 90 °C.[77] Hydroxyl groups of the cellulose were favorable sites for zeolite crystallization. Such zeolite coatings would be attractive for membrane separation applications.

Low molecular weight organic compounds that can gel solvents at low concentrations (organogelators) have been used to form hybrid, coated fibers and, upon the removal of the organic material, hollow inorganic fibers. A review of the different classes of organogelators and their physical properties is given by Terech and Weiss.[78] Generally, the gelator is dissolved by heating it in an organic liquid and then cooling to produce a gel- or jelly-like material due to fibrous aggregation of the gelator. When inorganic precursor molecules are added to the solution, inorganic oligomers grow on the surface of the gelator structures because of electrostatic attraction or hydrogen bonding. Hence, the organic superstructures that are held together by noncovalent interactions can be permanently fixed in inorganic materials.

A novel use of such gelators for the production of hybrid inorganic/organic fibers was reported in 1998[79] when the polymerization of TEOS was gelled by a cholesterol-based molecule with quaternary ammonium groups. The cationic groups played an essential role in the coating procedure. The anionic silica oligomers adsorbed onto the cationic gelator fibrils, and polymerization proceeded along the fibrils. After calcination, hollow silica fibers were formed; this was not the case when the same cholesterol gelator without quaternary ammonium groups was used. When a benzo-18-crown-6 containing cholesterol gelator was used during the silica polymerization, hollow fibers were only found when high concentrations of potassium perchlorate were added to the reaction.[80] This proved the electrostatic coupling between template and condensing silica. By variation of the salt concentration and the appended crown ether (monobenzo-18-crown-6, monoaza-18-crown-6, and 1,10-diaza-18-crown-6) on the cholesterol-based gelators, different organogel superstructures and hence silica structures were obtained.[81,82] The final silica materials were tubular in structure with either rough, irregular surfaces and thick walls (monobenzo-18-crown-6) or a smooth-surfaced, thin-walled, rolled paperlike structure (monoaza-18-crown-6 and 1,10-diaza-18-crown-6). Chiral spiral silica could also be formed (both right- and left-handed) when organogels consisting of chiral diaminocyclohexane derivatives were used as the template during sol−gel polymerization.[83,84] The transcription of "gemini"-type cholesterol-based gelator superstructures into silica showed that the templating effect can also occur through hydrogen-bonding interactions.[85]

Titania hybrid fibers have also been formed using organogel templates, as shown in the scanning electron microscopy image in Figure 7a. Fibrous aggregates of *trans*-(1*R*,2*R*)-1,2-cyclohexane di(11-aminocarbonylundecyl pyridinium) hexafluorophosphate, an amphiphilic compound containing cationic moieties, have been used to form hollow titanium dioxide fibers.[86] Calcination at 450 °C completely removed the organic compound (observed from FT-IR spectra), leaving hollow titania structures. SEM showed outer diameters of 150−600 nm, inner diameters of 50−300 nm, and maximum lengths of ≈200 μm (Figure 7b) when a base catalyst was used.

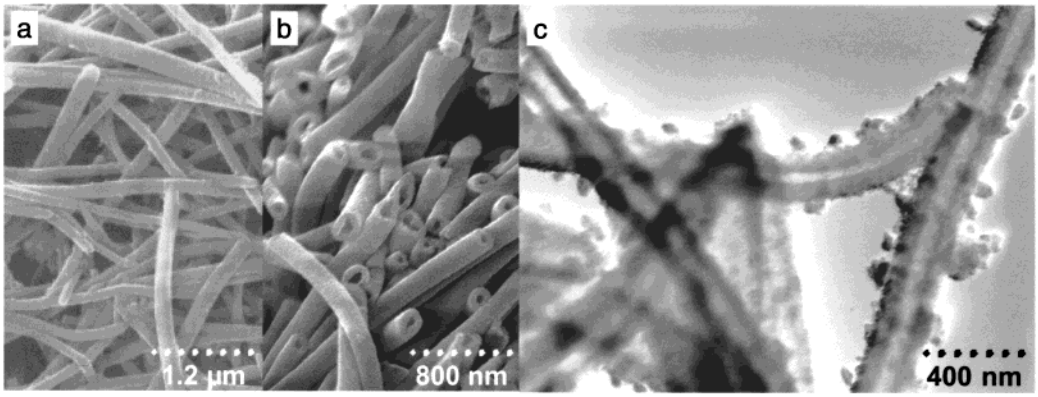

Figure 7. (a) SEM image of a dried titanium dioxide-coated gelator sample prepared under basic conditions, (b) SEM, and (c) TEM images of the hollow fibers formed after removal of the organic material by calcination. Reprinted in part with permission from ref 86. Copyright 2000 American Chemical Society.

The hollow, anatase phase fibers were also viewed by using TEM (Figure 7c). There is potential for these materials in a variety of photoelectric applications.

When *N*-carbobenzyloxy-L-isoleucylaminooctadecane was used, titanium isopropoxide was gelled through hydrogen-bonding interactions with the amine groups on the organic compound.[87] After drying of a 3-D network of the hybrid material, coated gelator fibers (diameter, 300−1500 nm) were obtained. Complete removal of the gelator is achieved by heating the hybrid to 450 °C, resulting in TiO_2 fibers (diameter 200−1200 nm, that is, there is slight shrinkage during the heating process), consisting of nanoparticles 15−30 nm in diameter of both anatase and rutile crystal structure, suggesting interaction of the titania oligomers with the gelator fibers. Potential applications for these titania hollow fibers are photovoltaics and photocatalysis.

Jung et al. have recently used vesicular aggregates of crown-appended cholesterol derivatives in organic solvents as templates.[88] Electron microscopy studies of the organogel structures showed spherical vesicles with two distinct diameters, ≈200 and ≈2500 nm with the smaller vesicles being linked like a "pearl necklace". The shell wall is made up of multilayers about 5-nm-thick, which can be correlated to the width of interdigitated folded azobenzene−cholesterol bilayers. Conducting a silica sol−gel reaction in these gel phases resulted in spherical silica structures (both isolated large diameter spheres, ≈2500 nm, and interconnected smaller spheres, ≈200 nm). After calcination and removal of the organic material, hollow spherical structures with walls that consist of multilayered lamella with ≈5-nm spacing were observed. This shows the preciseness of the silica coating technique.

Porous silica networks have been formed with two different pore sizes (several nanometers and several micrometers).[89] Here, 2,3-di-*n*-decyloxyanthracene was used as the gelator in methanol; the fibrous aggregates act as a template for the porous silica fibers while smaller aggregates induce mesoporosity. Variation in gelator concentration alters the mesopore diameters from 5 to 12 nm and the pore shape from ink bottle to cylindrical.

As in the case of the crystal templates, optimization to form uniform diameter fibers will enhance the areas of application of the final product by the fabrication of single-diameter hollow materials.

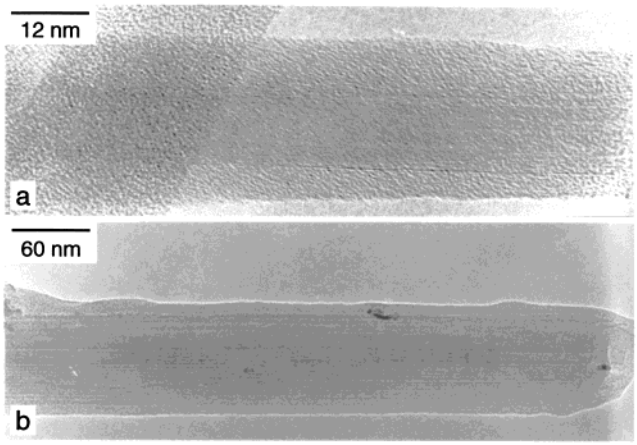

Figure 8. TEM images of (a) a zirconia-coated carbon nanotube and (b) a carbon nanotube coated with stabilized zirconia. Reprinted with permission from ref 90. Copyright 1997 The Royal Society of Chemistry.

5. Carbon Nanotubes

Carbon nanotube templates have been used for the production of zirconia and yttria-stabilized zirconia nanotubes.[90] The multiwalled carbon nanotubes were heat-treated, refluxed in concentrated nitric acid, and then reacted with zirconium propoxide in an argon atmosphere (Figure 8). After washing and drying, the sample was heated to 700 °C to oxidize the carbon. From electron microscopy analysis the final inorganic materials had a diameter of about 40 nm, a wall thickness of about 6 nm, and length of several micrometers. The zirconia was a 50:50 mix of both monoclinic and tetragonal phase. Heating to higher temperatures to obtain monophasic material resulted in collapse of the nanotubes. Hence, yttria was added in a modified procedure that produced nanotubes of yttria-stabilized zirconia (cubic phase).[90]

Previous work using the carbon nanotube templates by Rao and co-workers[91] led to SiO_2, Al_2O_3, and V_2O_5 nanotubes. The silica coating was obtained by stirring the carbon nanotubes in TEOS (12 h) and then heating initially in a vacuum at 100 °C followed by 500 °C in air. For the Al_2O_3 and V_2O_5 coatings the nanotubes were stirred in a gel of aluminum isopropoxide and water or a vanadium pentoxide gel, respectively. After washing and heating (500 and 450 °C), the Al_2O_3- and V_2O_5-coated carbon nanotubes were obtained. Heating to 750

°C under air oxidized the carbon, leaving nanotubes of SiO_2 and Al_2O_3. V_2O_5 assists in oxidizing the carbon; hence, lower temperatures (500 °C) resulted in V_2O_5 nanotubes. Transistion-metal ions were added to the silica-coated nanotubes by mixing the carbon nanotubes in a TEOS/ethanol solution containing transition-metal compounds. After the drying and heating procedures, silica nanotubes with small percentages of the transition-metal oxides (Ni, Cr, Cu, or Co) were obtained.[91] Coating carbon nanotubes with other oxides (WO_3, MoO_3, Sb_2O_5, MoO_2, RuO_2, and IrO_2) led generally to the formation of single-crystalline nanorods, with lengths up to a few micrometers and diameters ranging from 10 to 200 nm, after heating in air to 500 or 700 °C.[92]

6. Biomaterials

Biological materials with interesting self-assembled structures are attractive templates for coating procedures. The sensitivity of such templates to various reaction parameters makes the sol−gel process an appealing procedure for coating these materials.

The use of self-assembled lipids for sol−gel templating results in ceramic rods or hollow cylinders with a diameter of 500 nm.[93] Silane coating can also be used to change the chemical nature of the tubule surface. Diacetylenic phosphatidylcholine has been used to form helical silica-lipid structures by simultaneous phospholipid crystallization and silica polymerization.[94] This same phospholipid has been used to form silica tubes by coating the preformed phospholipid template.[95]

The tobacco mosaic virus has been used as a template for the formation of a number of inorganic−organic hybrid nanotubes.[96] The hollow protein tube with an inner diameter of 4 nm has outer dimensions of 300 × 18 nm and is relatively pH-stable. Hence, coating of the virus with SiO_2, CdS, PbS, and iron oxide with reaction pHs ranging from 2.5 to 9 was possible. A thin silica shell (3 nm) forms along the length of the outer virion surface, and end-to-end self-assembly of the nanotubes gave hybrid materials several times the length of the single tobacco mosaic virus (Figure 9).

The macroporous structure of demineralized cuttlebone, a β-chitin organic framework, has been coated with silica by soaking it in sodium silicate solutions at room temperature, followed by immersion in a series of ethanol/water mixtures and then an ethanol/ammonium hydroxide mixture.[97] The coating roughness was increased by increasing the supersaturation of the silica, and the thickness increased by increasing the level of deacetylation in the organic matrix prior to the coating procedure.

7. Membranes

Membranes consisting of cylindrical pores and bicontinuous networks of pores have been used as templates for the formation of hybrid materials as well as inorganic tubes and porous structures.

7.1. Alumina Membranes. Anodic porous alumina has uniformly sized, cylindrical pores with diameters ranging from 4 to 200 nm.[98] With fine control of the anodizing voltage and etching procedure during the film formation, the pores can be arranged in a regular honeycomb fashion.[99] Their structures have been used as templates by numerous groups to form both tubes and rods or aligned nanotubes or nanofibers that are fixed to a thin layer of excess final material at one end of the tubes/fibers.

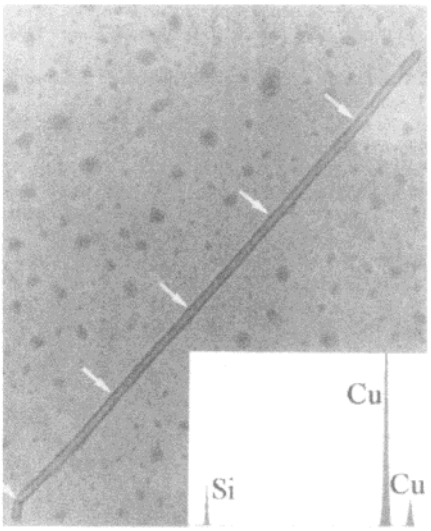

Figure 9. TEM image of the self-assembled silica-coated tobacco mosaic virus superstructure. The white arrows mark the ends of five individual TMV particles, each 300 nm in length, that have aggregated end-to-end along with a thin external shell of amorphous silica. Inset: Corresponding EDX spectrum showing Si peak (Cu peaks are from TEM grid). Reprinted with permission from ref 96. Copyright 1999 Wiley-VCH.

Template synthesis using membranes with cylindrical channels of uniform diameter has been well-studied.[100] Tubes of TiO_2 and ZnO have been prepared by immersing alumina membranes with a thickness of 50 μm and pore diameter of 200 nm into the titania and zinc oxide sol−gel solutions, respectively, followed by drying and heating.[101] The length of time of the immersion step (5 to 60 s) as well as the temperature (5 to 20 °C) of the sol−gel solution influence the final structure obtained: tubular with shorter immersion times and colder solutions compared with fibers for either longer immersion times or warmer solutions. The TiO_2 tubes have been surface-activated by attaching Sn^{2+} to the inner walls and used to immobilize enzyme, hence opening the possibility for bioreactor applications.[102] Upon removal of the alumina template, by immersion in aqueous base, the monodisperse metal oxide tubular structures with predetermined diameter and length (dependent on the membrane) can be collected as free individual entities or assembled together like bristles of a brush.

7.2. Polymer Membranes. Two simple procedures using cellulose acetate membranes and sol−gel processes have led to the formation of titanium and zirconium dioxide porous films.[103] The membrane was either soaked in the metal alkoxide precursor and then soaked in water/alcohol mixtures for hydrolysis/condensation reactions to occur or the precursor and then water/alcohol solution were filtered through the membrane. The amorphous metal oxide/cellulose acetate membrane was then heated to remove the organic material, leaving a film (≈80 μm in thickness) of a highly porous metal oxide (Figure 10). This structure was composed of crystalline nanoparticles, with their size and crystal phase dependent on the initial pore size

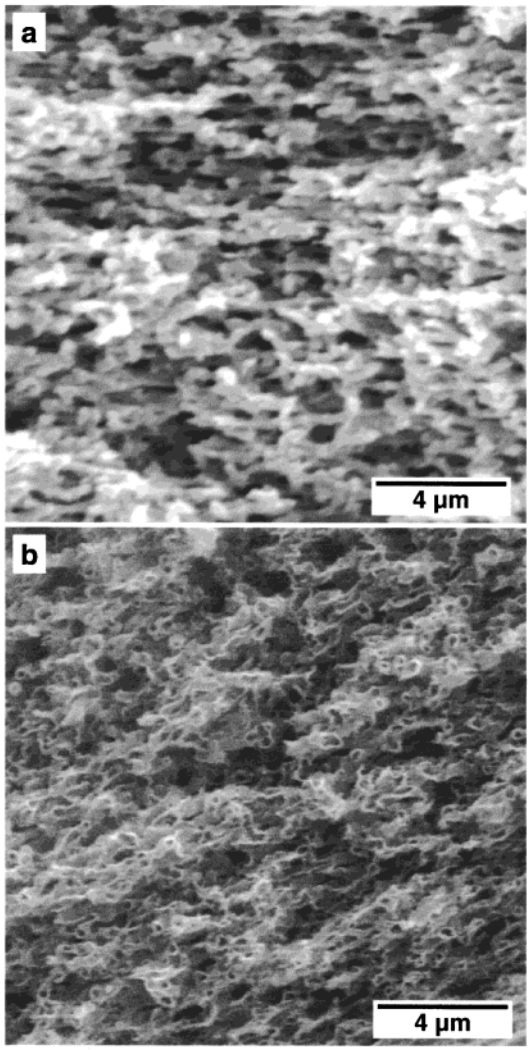

Figure 10. SEM images of (a) the cellulose acetate membrane template and (b) the final inorganic (ZrO_2) network formed after sol−gel coating of the template. Reprinted with permission from ref 103. Copyright 2000 Wiley-VCH.

of the membrane, the metal alkoxide precursor used, and the temperature of the heating process. Photovoltaics and photocatalysis are two areas where porous titania films could be applied.

7.3. Polymer Gels. Polymer gels are materials with similar bicontinuous structures to polymer membranes and have also been used as templates. Polymer gels can be tailored in a wide range with respect to their pore size/structure, overall structure/morphology, functionality, and physical properties.[104,105]

Sol−gel processes within polymer gels have led to the formation of hybrid inorganic/organic monoliths: The amorphous metal oxide coated the polymer gel surfaces, and upon removal of the polymer a highly porous, "coral-like" titanium dioxide network remained.[106] The pore size, when an acrylamide/glycidyl methacrylate polymer gel template was used, ranged from 100 nm to micrometers in diameter, and the coating thickness was 100−150 nm. The walls were comprised of titanium dioxide nanoparticles connected in continuous ribbons throughout the structure. Either anatase or rutile phase titanium dioxide could be achieved depending on the temperature used during calcination. Numerous other polymer gels have also been used as templates for titanium dioxide and zirconium dioxide network fabrication.[107] Changes in polymer pore structure and overall morphology are mimicked by the metal oxide network. Porous, high surface area materials (up to 100 $m^2\ g^{-1}$) have been achieved for titanium dioxide using this technique. Catalytic applications as well as catalyst supports are areas where these highly porous, monolithic structures have potential.

A sequence of coating procedures can also be carried out in the polymer gel.[107] A noncontinuous first layer can be deposited as single particles on the gel prior to a second continuous layer, resulting in nanoparticles enclosed within the second material. Platinum nanoparticles were first formed by reducing hydrogen hexachloroplatinate(IV) hydrate within the gel. Then, the titanium alkoxide sol−gel process was carried out, followed by calcination, resulting in a homogeneous distribution of platinum particles within the porous titanium dioxide network.

8. Summary and Outlook

Nanocoating techniques lead to the synthesis of novel functional materials with properties that depend on the combination of components employed in the fabrication process. Materials with specific applications can be designed by careful choice of the components and template morphology. Catalysis, electronics, biomaterials engineering, and materials chemistry are areas that will benefit from designed materials with specific functionality, and controlled arrangement or organization of the pore structures and particles, and their size.

Inorganic particles with dimensions ranging from nanometers to micrometers have been successfully coated using sol−gel processes. In the majority of cases the coatings are applied to enhance the properties of either the core or the coated material. Organic spherical templates have been coated with various inorganic layers, resulting in monodisperse particles with inorganic surface functionality but lower density than a complete inorganic particle. The ability to remove the inner core affords hollow inorganic materials with a range of applications.

Nanocoating has also been applied to elongated templates, such as crystals and fibers. The examples discussed in this review have shown that crystals can be coated to form composite materials and hollow structures with inner dimensions dependent on the crystal morphology. It has also been demonstrated that crystal coating is an efficient way to load a material, such as metal, within the tube formed by sol−gel processing. Coating of fibers leads to thermal stabilization of inorganic materials as well as the formation of hollow fiber materials when organic fibers are used as templates. Tubes also result from the coating of carbon nanotubes.

Lipids and macroporous demineralized cuttlebone are examples of biomaterials that can be coated, hence showing the importance of biological templatable materials for directing structured inorganic materials to form interesting fibers and complex three-dimensional networks. The coating of such bicontinuous networks has also been achieved by using polymer templates of both monolithic and thin film form. These highly porous materials are expected to perform well in mass-transfer

applications. The simplicity of such complex structure formation in itself makes it an attractive process.

One of the main challenges in coating nanostructured templates is to achieve a homogeneous layer of the inorganic material without the formation of free (excess) inorganic particles in solution. Therefore, considerable effort goes into controlling the adhesion of the inorganic coating via the reaction conditions, thereby optimizing the coating quality while preventing disruption or aggregation of the template, and preventing the presence of noncoating inorganic material.

The majority of the templates used in the coating procedures have reached a stage where they can be formed with monodisperse size (colloid particles) or of consistent morphology (membrane pore structure, for example); however, crystals and fibers could be further optimized to form starting materials with uniform properties. Control of the coating thickness so that it can be finely tuned is of utmost importance when applications are to be considered. Hence, reaction conditions need to be carefully monitored and well-documented to allow reproducible coatings. Ordering of the initial templates or the coated template, in the form of aligned rods and fibers, or crystals of coated colloid particles will allow many of the perceived applications to reach fruition. Much of this work is already in progress and in the not too distant future we will see numerous nanocoated materials achieving exciting results in different areas of application.

Acknowledgment. The Max Planck Society is thanked for financial support.

References

(1) Brinker, C. J.; Scherer, G. W. *Sol−Gel Science: The Physics and Chemistry of Sol−Gel Processing*; Academic Press: San Diego, 1990.
(2) Stein, A.; Melde, B. J.; Schroden, R. C. *Adv. Mater.* **2000**, *12*, 1403−1419.
(3) Fullam, S.; Cottell, D.; Rensmo, H.; Fitzmaurice, D. *Adv. Mater.* **2000**, *12*, 1430−1433.
(4) Govindaraj, A.; Satishkumar, B. C.; Nath, M.; Rao, C. N. R. *Chem. Mater.* **2000**, *12*, 202−205.
(5) Pan, S. L.; Zeng, D. D.; Zhang, H. L.; Li, H. L. *Appl. Phys. A* **2000**, *70*, 637−640.
(6) Pender, M. J.; Sneddon, L. G. *Chem. Mater.* **2000**, *12*, 280−283.
(7) Göltner, C. G.; Berton, B.; Krämer, E.; Antonietti, M. *Adv. Mater.* **1999**, *11*, 395−398.
(8) Imhof, A.; Pine, D. J. *Adv. Mater.* **1999**, *11*, 311−314.
(9) Li, Y.; Xu, D.; Zhang, Q.; Chen, D.; Huang, F.; Xu, Y.; Guo, G.; Gu, Z. *Chem. Mater.* **1999**, *11*, 3433−3435.
(10) Patrissi, C. J.; Martin, C. R. *J. Electrochem. Soc.* **1999**, *146*, 3176−3180.
(11) Ying, J. Y.; Mehnert, C. P.; Wong, M. S. *Angew. Chem., Int. Ed.* **1999**, *38*, 56−77.
(12) Zhang, Z.; Gekhtman, D.; Dresselhaus, M. S.; Ying, J. Y. *Chem. Mater.* **1999**, *11*, 1659−1665.
(13) Krämer, E.; Förster, S.; Göltner, C.; Antonietti, M. *Langmuir* **1998**, *14*, 2027−2031.
(14) Yang, P.; Deng, T.; Zhao, D.; Feng, P.; Pine, D.; Chmelka, B. F.; Whitesides, G. M.; Stucky, G. D. *Science* **1998**, *282*, 2244−2246.
(15) Yang, P.; Zhao, D.; Margolese, D. I.; Chmelka, B. F.; Stucky, G. D. *Nature* **1998**, *396*, 152−155.
(16) Zhao, D.; Feng, J.; Huo, Q.; Melosh, N.; Fredrickson, G. H.; Chmelka, B. F.; Stucky, G. D. *Science* **1998**, *279*, 548−552.
(17) Hornyak, G. L.; Patrissi, C. J.; Martin, C. R. *J. Phys. Chem. B* **1997**, *101*, 1548−1555.
(18) Imhof, A.; Pine, D. J. *Nature* **1997**, *389*, 948−951.
(19) Weissenberger, M. C.; Göltner, C. G.; Antonietti, M. *Ber. Bunsen-Ges. Phys. Chem.* **1997**, *101*, 1679−1682.
(20) Bagshaw, S. A.; Prouzet, E.; Pinnavaia, T. J. *Science* **1995**, *269*, 1242−1244.
(21) Bognitzki, M.; Hou, H.; Ishaque, M.; Frese, T.; Hellwig, M.; Schwarte, C.; Schaper, A.; Wendorff, J. H.; Greiner, A. *Adv. Mater.* **2000**, *12*, 637−640.
(22) Breulmann, M.; Davis, S. A.; Mann, S.; Hentze, H.-P.; Antonietti, M. *Adv. Mater.* **2000**, *12*, 502−507.
(23) Caruso, F. *Chem. Eur. J.* **2000**, *6*, 413−419.
(24) Zhang, B.; Davis, S. A.; Mendelson, N. H.; Mann, S. *Chem. Commun.* **2000**, 781−782.
(25) Subramanian, G.; Manoharan, V. N.; Thorne, J. D.; Pine, D. J. *Adv. Mater.* **1999**, *11*, 1261−1265.
(26) Caruso, F.; Lichtenfeld, H.; Giersig, M.; Möhwald, H. *J. Am. Chem. Soc.* **1998**, *120*, 8523−8524.
(27) Caruso, F.; Caruso, R. A.; Möhwald, H. *Science* **1998**, *282*, 1111−1114.
(28) Davis, S. A.; Patel, H. M.; Mayes, E. L.; Mendelson, N. H.; Franco, G.; Mann, S. *Chem. Mater.* **1998**, *10*, 2516−2524.
(29) Davis, S. A.; Burkett, S. L.; Mendelson, N. H.; Mann, S. *Nature* **1997**, *385*, 420−423.
(30) Caruso, F. *Adv. Mater.* **2001**, *13*, 11−22.
(31) Philipse, A. P.; van Bruggen, M. P. B.; Pathmamanoharan, C. *Langmuir* **1994**, *10*, 92−99.
(32) Liz-Marzán, L. M.; Giersig, M.; Mulvaney, P. *Langmuir* **1996**, *12*, 4329−4335.
(33) Correa-Duarte, M. A.; Giersig, M.; Liz-Marzán, L. M. *Chem. Phys. Lett.* **1998**, *286*, 497−501.
(34) Mulvaney, P.; Liz-Marzán, L. M.; Giersig, M.; Ung, T. *J. Mater. Chem.* **2000**, *10*, 1259−1270.
(35) Alejandro-Arellano, M.; Ung, T.; Blanco, Á.; Mulvaney, P.; Liz-Marzán, L. M. *Pure Appl. Chem.* **2000**, *72*, 257−267.
(36) Aliev, F. G.; Correa-Duarte, M. A.; Mamedov, A.; Ostrander, J. W.; Giersig, M.; Liz-Marzán, L. M.; Kotov, N. A. *Adv. Mater.* **1999**, *11*, 1006−1010.
(37) Giersig, M.; Ung, T.; Liz-Marzán, L. M.; Mulvaney, P. *Adv. Mater.* **1997**, *9*, 570−575.
(38) Oldfield, G.; Ung, T.; Mulvaney, P. *Adv. Mater.* **2000**, *12*, 1519−1522.
(39) Pastoriza-Santos, I.; Koktysh, D. S.; Mamedov, A. A.; Giersig, M.; Kotov, N. A.; Liz-Marzán, L. M. *Langmuir* **2000**, *16*, 2731−2735.
(40) Stöber, W.; Fink, A.; Bohn, E. *J. Colloid Interface Sci.* **1968**, *26*, 62−69.
(41) Hardikar, V. V.; Matijević, E. *J. Colloid Interface Sci.* **2000**, *221*, 133−136.
(42) Adair, J. H.; Li, T.; Kido, T.; Havey, K.; Moon, J.; Mecholsky, J.; Morrone, A.; Talham, D. R.; Ludwig, M. H.; Wang, L. *Mater. Sci. Eng. Rep.* **1998**, *R23*, 139−242.
(43) Li, T.; Moon, J.; Morrone, A. A.; Mecholsky, J. J.; Talham, D. R.; Adair, J. H. *Langmuir* **1999**, *15*, 4328−4334.
(44) Ryan, J. N.; Elimelech, M.; Baeseman, J. L.; Magelky, R. D. *Environ. Sci. Technol.* **2000**, *34*, 2000−2005.
(45) Garg, A.; Matijević, E. *J. Colloid Interface Sci.* **1988**, *126*, 243−250.
(46) Aiken, B.; Matijević, E. *J. Colloid Interface Sci.* **1988**, *126*, 645−649.
(47) Garg, A.; Matijević, E. *Langmuir* **1988**, *4*, 38−44.
(48) Ohmori, M.; Matijević, E. *J. Colloid Interface Sci.* **1992**, *150*, 594−598.
(49) ul Haq, I.; Matijević, E. *J. Colloid Interface Sci.* **1997**, *192*, 104−113.
(50) Hsu, W. P.; Yu, R.; Matijević, E. *J. Colloid Interface Sci.* **1993**, *156*, 56−65.
(51) Ocaña, M.; Hsu, W. P.; Matijević, E. *Langmuir* **1991**, *7*, 2911−2916.
(52) Haq, I.; Matijević, E. *Colloids Surf. A* **1993**, *81*, 153−159.
(53) Aiken, B.; Hsu, W. P.; Matijević, E. *J. Mater. Sci.* **1990**, *25*, 1886−1894.
(54) Giesche, H.; Matijević, E. *J. Mater. Res.* **1994**, *9*, 436−450.
(55) Srinivasan, S.; Datye, A. K.; Hampden-Smith, M.; Wachs, I. E.; Deo, G.; Jehng, J. M.; Turek, A. M.; Peden, C. H. F. *J. Catal.* **1991**, *131*, 260−275.
(56) Hanprasopwattana, A.; Srinivasan, S.; Sault, A. G.; Datye, A. K. *Langmuir* **1996**, *12*, 3173−3179.
(57) Guo, X.-C.; Dong, P. *Langmuir* **1999**, *15*, 5535−5540.
(58) Wang, G.; Harrison, A. *J. Colloid Interface Sci.* **1999**, *217*, 203−207.
(59) Kawahashi, N.; Matijević, E. *J. Colloid Interface Sci.* **1990**, *138*, 534−542.
(60) Kawahashi, N.; Persson, C.; Matijević, E. *J. Mater. Chem.* **1991**, *1*, 577−582.
(61) Shiho, H.; Kawahashi, N. *Colloid Polym. Sci.* **2000**, *278*, 270−274.
(62) Bamnolker, H.; Nitzan, B.; Gura, S.; Margel, S. *J. Mater. Sci. Lett.* **1997**, *16*, 1412−1415.
(63) Holland, B. T.; Blanford, C. F.; Stein, A. *Science* **1998**, *281*, 538−540.
(64) Holland, B. T.; Blanford, C. F.; Do, T.; Stein, A. *Chem. Mater.* **1999**, *11*, 795−805.
(65) Park, S. H.; Xia, Y. *Adv. Mater.* **1998**, *10*, 1045−1048.
(66) Gates, B.; Yin, Y.; Xia, Y. *Chem. Mater.* **1999**, *11*, 2827−2836.
(67) Tamon, H.; Sone, T.; Mikami, M.; Okazaki, M. *J. Colloid Interface Sci.* **1997**, *188*, 493−500.
(68) Wijnhoven, J. E. G. J.; Vos, W. L. *Science* **1998**, *281*, 802−804.

(69) Yan, H.; Blanford, C. F.; Holland, B. T.; Parent, M.; Smyrl, W. H.; Stein, A. *Adv. Mater.* **1999**, *11*, 1003−1006.
(70) Vlasov, Y. A.; Yao, N.; Norris, D. J. *Adv. Mater.* **1999**, *11*, 165−169.
(71) Zhong, Z.; Yin, Y.; Gates, B.; Xia, Y. *Adv. Mater.* **2000**, *12*, 206−209.
(72) Hippe, C.; Wark, M.; Lork, E.; Schulz-Ekloff, G. *Microporous Mesoporous Mater.* **1999**, *31*, 235−239.
(73) Nakamura, H.; Matsui, Y. *J. Am. Chem. Soc.* **1995**, *117*, 2651−2652.
(74) Nakamura, H.; Matsui, Y. *Adv. Mater.* **1995**, *7*, 871−872.
(75) Miyaji, F.; Davis, S. A.; Charmant, J. P. H.; Mann, S. *Chem. Mater.* **1999**, *11*, 3021−3024.
(76) Dong, R.; Hirata, Y. *J. Ceram. Soc. Jpn.* **2000**, *108*, 823−829.
(77) Valtchev, V.; Mintova, S.; Vulchev, I.; Lazarova, V. *J. Chem. Soc., Chem. Commun.* **1994**, 2087−2088.
(78) Terech, P.; Weiss, R. G. *Chem. Rev.* **1997**, *97*, 3133−3159.
(79) Ono, Y.; Nakashima, K.; Sano, M.; Kanekiyo, Y.; Inoue, K.; Hojo, J.; Shinkai, S. *Chem. Commun.* **1998**, 1477−1478.
(80) Ono, Y.; Kanekiyo, Y.; Inoue, K.; Hojo, J.; Shinkai, S. *Chem. Lett.* **1999**, 23−24.
(81) Jung, J. H.; Ono, Y.; Shinkai, S. *J. Chem. Soc., Perkin Trans. 2* **1999**, 1289−1291.
(82) Jung, J. H.; Ono, Y.; Shinkai, S. *Langmuir* **2000**, *16*, 1643−1649.
(83) Jung, J. H.; Ono, Y.; Shinkai, S. *Angew. Chem., Int. Ed.* **2000**, *39*, 1862.
(84) Jung, J. H.; Ono, Y.; Hanabusa, K.; Shinkai, S. *J. Am. Chem. Soc.* **2000**, *122*, 5008−5009.
(85) Jung, J. H.; Ono, Y.; Shinkai, S. *Chem. Lett.* **2000**, 636−637.
(86) Kobayashi, S.; Hanabusa, K.; Hamasaki, N.; Kimura, M.; Shirai, H.; Shinkai, S. *Chem. Mater.* **2000**, *12*, 1523−1525.
(87) Kobayashi, S.; Hanabusa, K.; Suzuki, M.; Kimura, M.; Shirai, H. *Chem. Lett.* **1999**, 1077−1078.
(88) Jung, J. H.; Ono, Y.; Sakurai, K.; Sano, M.; Shinkai, S. *J. Am. Chem. Soc.* **2000**, *122*, 8648−8653.
(89) Clavier, G. M.; Pozzo, J. L.; Bouas-Laurent, H.; Liere, C.; Roux, C.; Sanchez, C. *J. Mater. Chem.* **2000**, *10*, 1725−1730.
(90) Rao, C. N. R.; Satishkumar, B. C.; Govindaraj, A. *Chem. Commun.* **1997**, 1581−1582.
(91) Satishkumar, B. C.; Govindaraj, A.; Vogl, E. M.; Basumallick, L.; Rao, C. N. R. *J. Mater. Res.* **1997**, *12*, 604−606.
(92) Satishkumar, B. C.; Govindaraj, A.; Nath, M.; Rao, C. N. R. *J. Mater. Chem.* **2000**, *10*, 2115−2119.
(93) Schnur, J. M. *Science* **1993**, *262*, 1669−1676.
(94) Mann, S.; Burkett, S. L.; Davis, S. A.; Fowler, C. E.; Mendelson, N. H.; Sims, S. D.; Walsh, D.; Whilton, N. T. *Chem. Mater.* **1997**, *9*, 2300−2310.
(95) Baral, S.; Schoen, P. *Chem. Mater.* **1993**, *5*, 145−147.
(96) Shenton, W.; Douglas, T.; Young, M.; Stubbs, G.; Mann, S. *Adv. Mater.* **1999**, *11*, 253−256.
(97) Ogasawara, W.; Shenton, W.; Davis, S. A.; Mann, S. *Chem. Mater.* **2000**, *12*, 2835−2837.
(98) Masuda, H.; Fukuda, K. *Science* **1995**, *268*, 1466−1468.
(99) Masuda, H.; Yamada, H.; Satoh, M.; Asoh, H.; Nakao, M.; Tamamura, T. *Appl. Phys. Lett.* **1997**, *71*, 2770−2772.
(100) Hulteen, J. C.; Martin, C. R. Template Synthesis of Nanoparticles in Nanoporous Membranes; In *Nanoparticles and Nanostructured Films: Preparation, Characterization and Applications.*; Fendler, J. H., Ed.; Wiley-VCH: New York, 1998; pp 235−262.
(101) Lakshmi, B. B.; Dorhout, P. K.; Martin, C. R. *Chem. Mater.* **1997**, *9*, 857−862.
(102) Lakshmi, B. B.; Patrissi, C. J.; Martin, C. R. *Chem. Mater.* **1997**, *9*, 2544−2550.
(103) Caruso, R. A.; Schattka, J. H. *Adv. Mater.* **2000**, *12*, 1921−1923.
(104) Antonietti, M.; Göltner, C.; Hentze, H.-P. *Langmuir* **1998**, *14*, 2670−2676.
(105) Antonietti, M.; Caruso, R. A.; Göltner, C. G.; Weissenberger, M. C. *Macromolecules* **1999**, *32*, 1383−1389.
(106) Caruso, R. A.; Giersig, M.; Willig, F.; Antonietti, M. *Langmuir* **1998**, *14*, 6333−6336.
(107) Caruso, R. A.; Antonietti, M.; Giersig, M.; Hentze, H.-P.; Jia, J. *Chem. Mater.* **2000**, *13*, 1114−1123.

CM001257Z